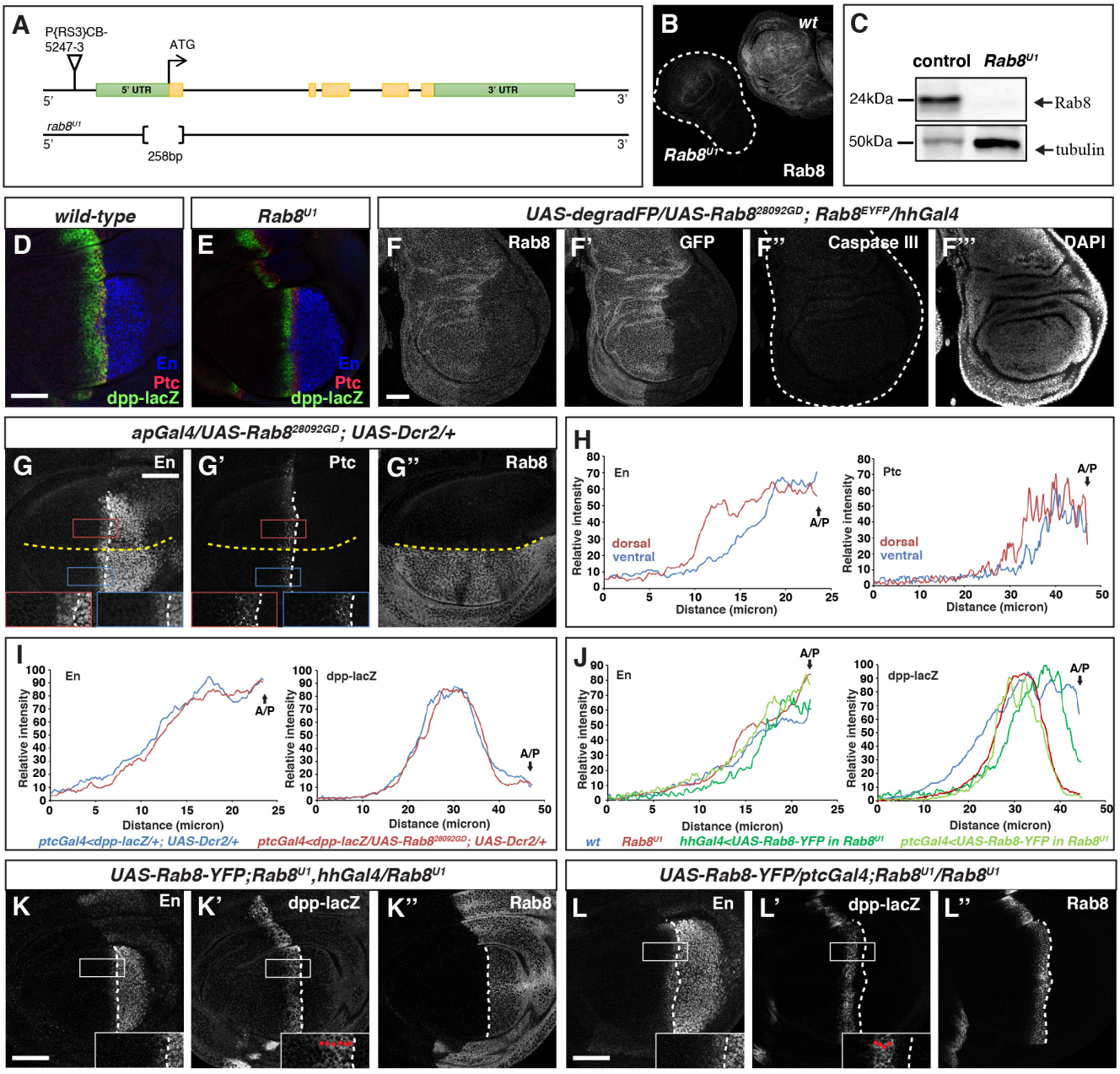

Figure S1. Validation of *Rab8* tools and the *Rab8^{U1}* mutant phenotype

A, map of the *Rab8* locus with the P-element insertion used for the P-element jump. B, *Rab8^{U1}* and wild-type discs co-stained in the same vial with anti-Rab8 antibody and imaged at the same time. C, Western-blot from wild-type and *Rab8^{U1}* whole larvae lysates revealed with anti-Rab8 antibody. D-E, additional example for a wild-type (D) and a *Rab8^{U1}* (E) mutant disc. F-F’’’, test of the RNAi/deGradFP system (for details see **Materials and Methods** and main text). Note that the anti-Rab8 signal is indistinguishable from the YFP staining (F,F’), and the conditional *Rab8* mutant tissue does not display any apoptotic defects (F’’,F’’’). G-G’’, expression of *Rab8* dsRNA in the dorsal compartment leads to En and Ptc expansion (compare red and blue insets on G and G’, representing the dorsal and the control ventral compartments, respectively). The yellow dashed line marks the D/V boundary. Dorsal is up and posterior is to the right. H, representative example (out of 20 discs quantified 15 shows this phenotype) for quantification of changes in Hh target expressions mentioned before. I, quantification of changes in Hh target expressions (En, *dpp-lacZ*) in *ptcGal4* control discs (n=8), and *Rab8* dsRNA expressing discs in the *ptc* domain (n=9). Note, that *Rab8* loss of function in anterior cells do not modify Hh target gene expression compared to the control. J-L’’, compartment specific rescue experiments. J, quantification of changes in Hh target expressions (En, *dpp-lacZ*) in wild-type, *Rab8^{U1}* mutant, and anterior or posterior specific rescue experiments. Note the partial restoration of En and *dpp-lacZ* expression, when wild-type Rab8 is re-expressed in Hh producing cells (dark green line). Note, that wild-type Hh target gene expression (E) is restored only, when the wild-type Rab8-YFP is expressed in Hh secreting cells (K-K’’). The *Rab8^{U1}* loss of function phenotype (E) is not rescued upon

expression of Rab8-YFP in anterior cells (L-L''). Insets in the bottom right corner on K, K' and L, L' are marked with white rectangle on the corresponding images. The A/P boundary (marked with white dashed line) is defined on K-L'' by the Rab8 signal (K'',L''). In D-G'' and K-L'' dorsal is up and posterior is to the right. The A/P boundary on H-J is indicated with black arrows. Scale bars: 50µm.

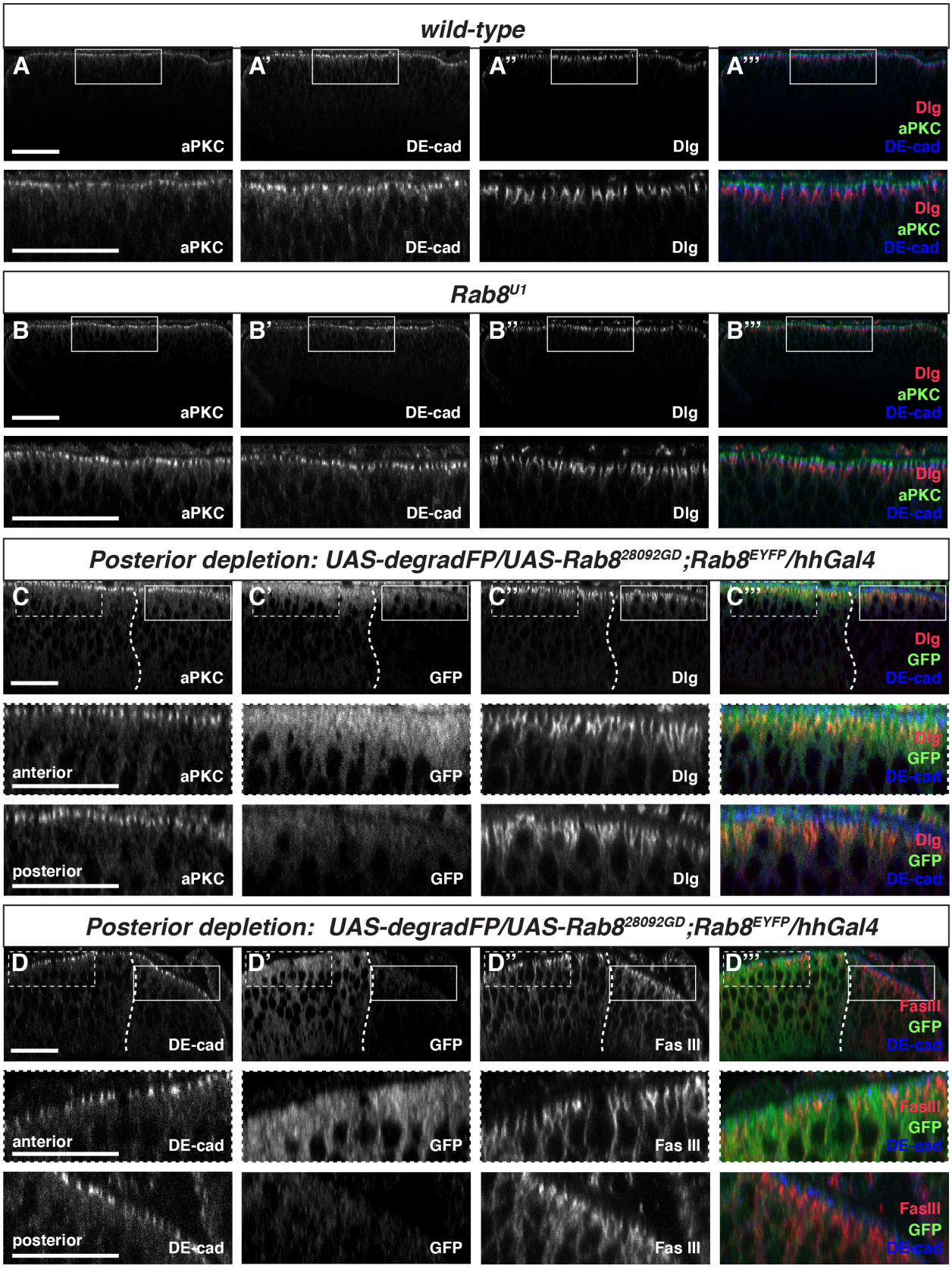

Figure S2. Subcellular distribution of polarity markers and Hh components in *Rab8* loss of function cells

A-B’’’, Single posterior Z-sections showing distribution of aPKC (A,B), DE-cadherin (A’, B’), and Dlg (A”, B”) in control (A), and $Rab8^{U1}$ mutant (B). C-C’’’, single Z sections along the A/P axis with aPKC (C), GFP (C’) and Dlg (C’’) in a RNAi/deGradFP disc. D-D’’’, single Z-sections showing DE-cad (D), GFP (D’), and FasciclinIII (D”) distribution in RNAi/deGradFP condition. Insets are magnified images of the area delimited with white rectangles (for posterior) or white dashed rectangles (for anterior) on the original images. (A’’’, B’’’, C’’’, D’’’) are merged images of the three channels. For all Z-sections apical is up. Posterior is to the right on C-D’’’. On C-D’’’ A/P compartment boundaries are marked with white dashed lines defined by the lack of GFP signal (C’,D’). Scale bars: 50µm.

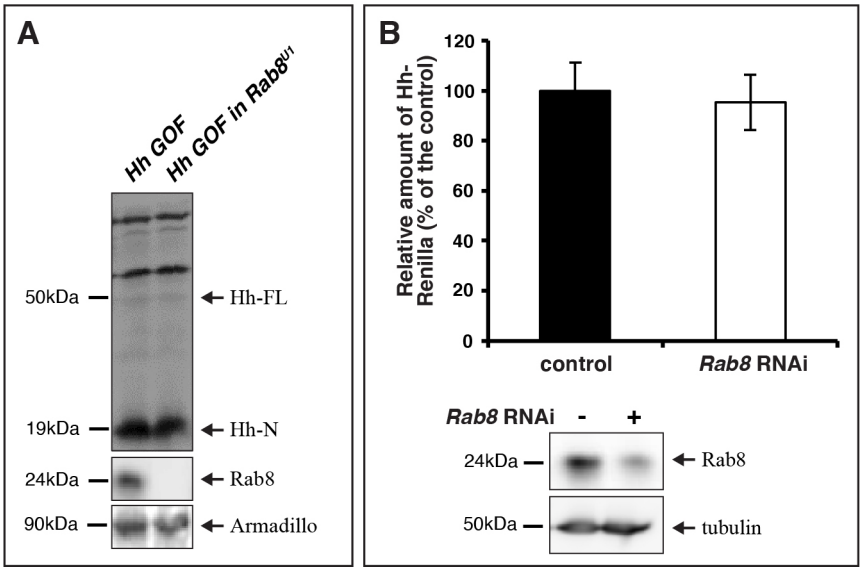

Figure S3. Hh level and secretion is not affected in absence of Rab8

A, Western-blot from control or *Rab8*^{U1} larvae probed with anti-Hh antibody. Note that Hh processing, or levels are not affected by the absence of Rab8. B, secretion of Hh-Renilla fusion protein from S2 cells into the culture media. Depletion of *Rab8* by RNAi in S2 cells does not decrease secretion of Hh-Renilla. This treatment leads to the reduction of Rab8 protein level by 60%.

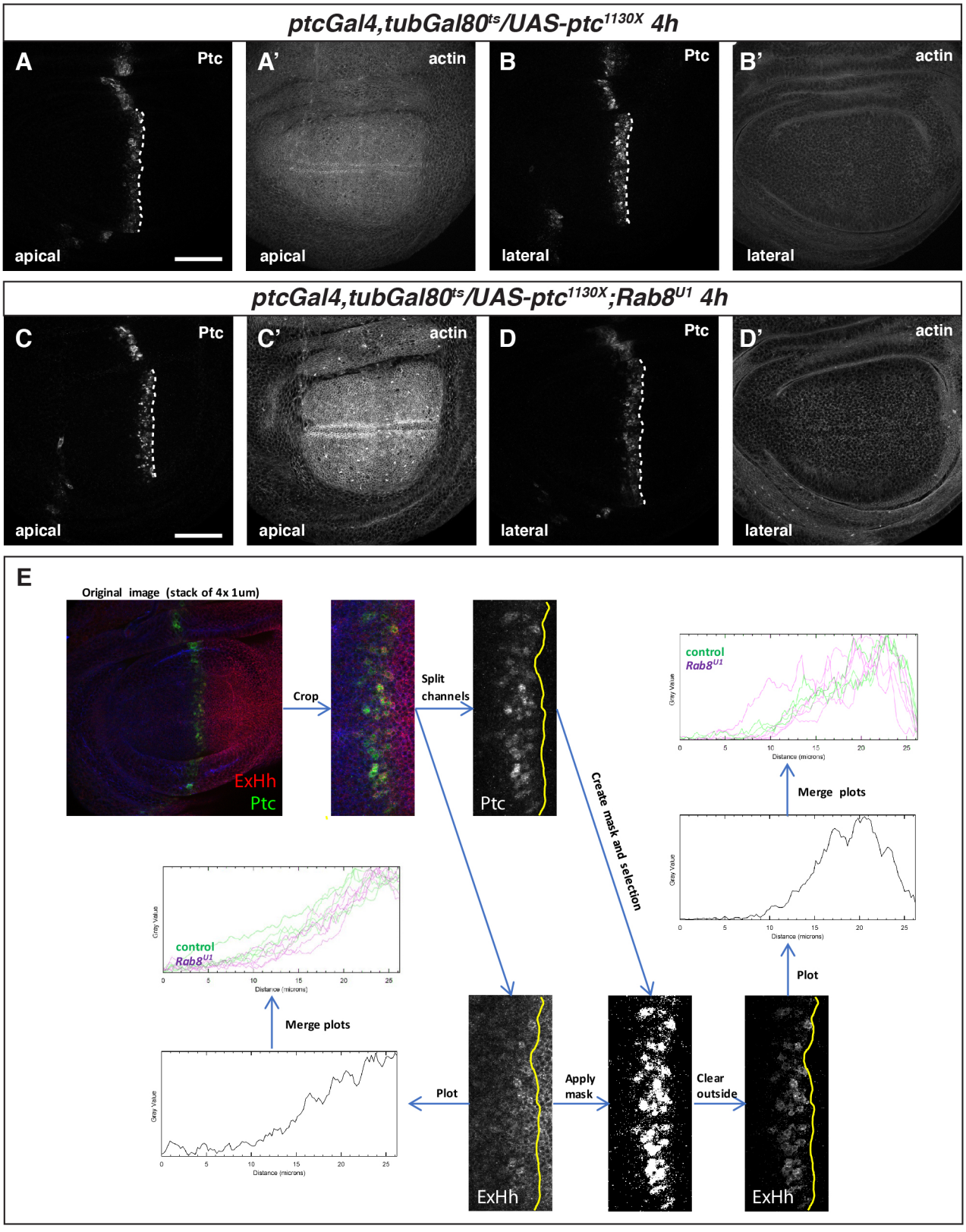

Figure S4. Additional confocal channels and quantification scheme for main Figure 4

A-D': A-A' correspond to **Figure 4C**, B-B' correspond to **Figure 4D**, C-C' correspond to **Figure 4E**, D-D' correspond to **Figure 4F**. In A' and C' the actin staining is enriched in two stripes which is due to an apical groove at the D/V border. Anterior is to the left, apical is up. Scale bars: 50µm. E, scheme of the quantification method used to measure Ptc^{1130X} bound Hh in wild-type and $Rab8^{U1}$ mutant backgrounds. A mask was created using the Ptc channel to restrain the quantification of released Hh to the Ptc domain. After applying the mask, all signal outside of this selection was cleared, which results in a drop of Hh signal at the A/P boundary (**Figure 4G**).

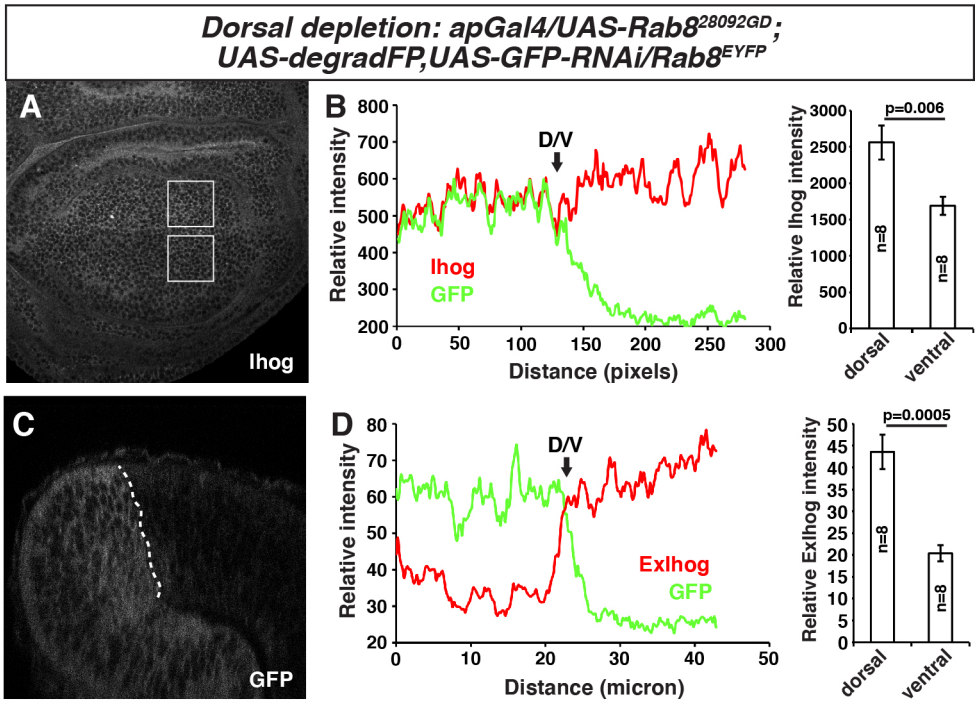

Figure S5. Quantifications for lateral Ihog intensity increase in RNAi/degradFP condition

A, The same disc as on **Figure 5A, 5A'**, the white rectangles mark the magnified areas presented on the insets of main **Figure 5A, 5A'**. B, quantification of intracellular Ihog staining intensities, dorsal versus ventral on RNAi/degradFP discs, p=0,006. C, GFP channel of the disc presented on main **Figure 5D, 5D'**. The D/V boundary is marked with white dashed line, defined by the lack of GFP signal (C). Dorsal is to the right, apical is up. D, quantification of extracellular Ihog staining intensities (n=8), dorsal versus ventral on RNAi/degradFP discs, p=0,0005. The D/V boundary is indicated with black arrows on B and D.

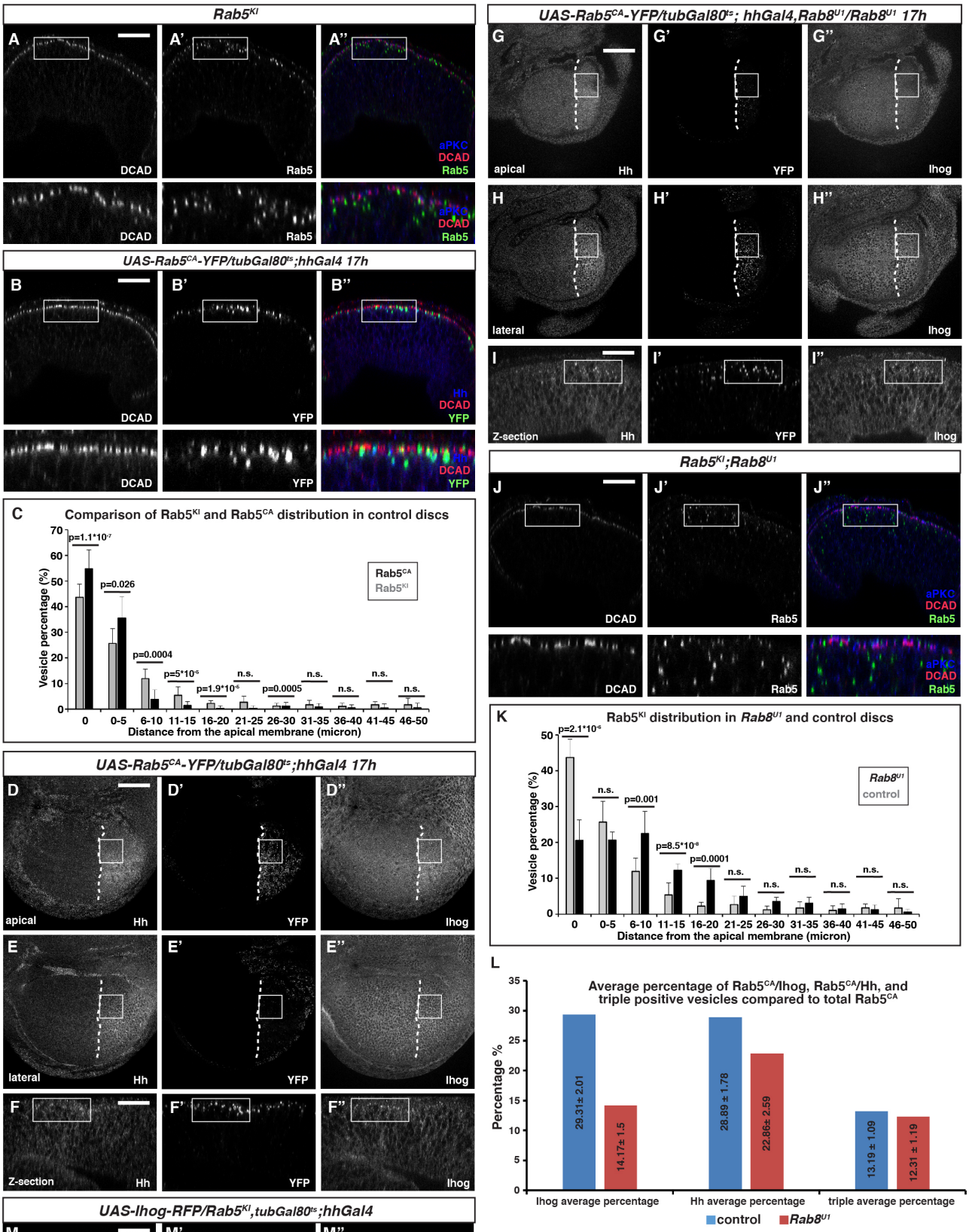

Figure S6. Additional confocal channels for main Figure 7, comparison of Rab5^{KI} and Rab5^{CA}-YFP distribution, and Rab5^{KI} distribution in the *Rab8^{U1}* mutant

A-C, comparison of Rab5^{KI} and Rab5^{CA}-YFP distribution in wild type background. For (C) Rab5^{CA}-YFP: n=313; Rab5^{KI}: n=602. D-I'', discs at low magnification corresponding to the images shown on **Figure 7**. The white rectangles depict the place of the crops presented on **Figure 7**. Dorsal is up and posterior is to the right. White dashed lines mark the A/P boundary, defined by the limit of Rab5^{CA}-YFP expression. Scale bars: 50µm. J-K, comparison of Rab5^{KI} distribution in wild type and *Rab8^{U1}* backgrounds. Note that, similar to Rab5^{CA}-YFP, Rab5^{KI} endosomes display a lateral shift in their localization in the *Rab8* mutant (compare A',A'' to J',J'' and K). For (K) Rab5^{KI} control: n=602; Rab5^{KI} in *Rab8^{U1}* mutant: n=725. The white rectangles on A-B'' and J-J'' depict the place of the crops presented below the corresponding panels. C and K: percentage of Rab5 positive endosomes are plotted relative to the apical marker in 5 micron increments. L, Quantification of Rab5^{CA}-YFP endosomes containing either Hh or Ihog or both in wild-type (control, n=3) or in *Rab8* mutant (*Rab8^{U1}*, n=5). In each disc 300 Rab5^{CA}-YFP vesicles were counted. Apical is up on all the images. M-M", Ihog overexpression in the posterior compartment in wild-type background. Rectangles depict posterior cells, and dashed rectangles mark anterior cells (magnifications are presented below the corresponding panels). Note that Ihog overexpression does not influence Rab5 subcellular distribution. The A/P boundary is defined by the anterior limit of IhogRFP expression (white dashed line). Apical is up and posterior is to the right. Scale bars: 50µm.

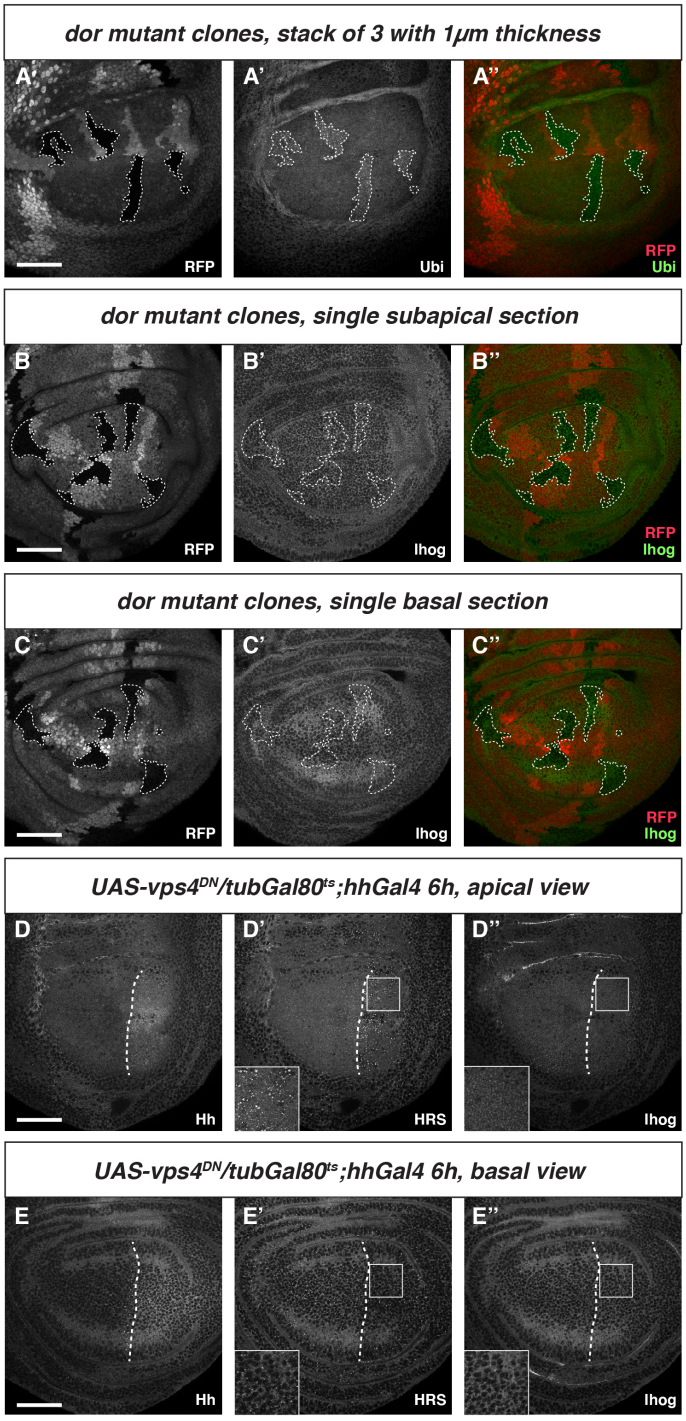

Figure S7. Ihog is not degraded in Hh producing cells

A-C, *dor* mutant clones labelled by the absence of RFP and stained for anti-Ubi epitopes (A',A") or Ihog (B',B", C',C"). Mutant clones are labelled by the absence of RFP (and marked with white dashed lines). D-E, posterior specific overexpression of $Vps4^{DN}$ for 6 hours leads to accumulation of HRS in maturation-deficient endosomes (D',E') but not of Ihog (D",E"). The A/P boundary is delimited with white dashed lines. Scale bars: 50 µm.